UPPSALA
UNIVERSITET

Digital Comprehensive Summaries of Uppsala Dissertations from the Faculty of Science and Technology 1559

Modelling of Moving Contact Lines in Two-Phase Flows

HANNA HOLMGREN

ACTA
UNIVERSITATIS
UPSALIENSIS
UPPSALA
2017

ISSN 1651-6214
ISBN 978-91-513-0071-9
urn:nbn:se:uu:diva-329059

Dissertation presented at Uppsala University to be publicly examined in ITC 2446, Lägerhyddsvägen 2, Uppsala, Friday, 27 October 2017 at 10:15 for the degree of Doctor of Philosophy. The examination will be conducted in English. Faculty examiner: Prof. Dr. Stefan Turek (Institute of Applied Mathematics (LSIII), TU Dortmund, Vogelpothsweg 87, D-44221 Dortmund, Germany).

Abstract

Holmgren, H. 2017. Modelling of Moving Contact Lines in Two-Phase Flows. *Digital Comprehensive Summaries of Uppsala Dissertations from the Faculty of Science and Technology* 1559. 33 pp. Uppsala: Acta Universitatis Upsaliensis. ISBN 978-91-513-0071-9.

Moving contact line problems appear in many natural and industrial processes. A contact line is formed where the interface between two immiscible fluids meets a solid wall. Examples from everyday life include raindrops falling on a window and water bugs resting on water surfaces. In many cases the dynamics of the contact line affects the overall behavior of the system. Industrial applications where the contact line behavior is important include gas and oil recovery in porous media, lubrication, inkjet printing and microfluidics. Computer simulations are fundamental tools to understand and predict the behavior.

In this thesis we look at numerical simulations of dynamic contact line problems. Despite their importance, the physics of moving contact lines is poorly understood. The standard Navier-Stokes equations together with the conventional no-slip boundary condition predicts a singularity in the shear stresses at the contact line. Atomistic processes at the contact line come into play, and it is necessary to include these processes in the model to resolve the singularity. In the case of capillary driven flows for example, it has been observed that the microscopic contact line dynamics has a large impact on the overall macroscopic flow.

In Paper I we present a new multiscale model for numerical simulation of flow of two immiscible and incompressible fluids in the presence of moving contact points (i.e. two-dimensional problems). The paper presents a new boundary methodology based on combining a relation between the apparent contact angle and the contact point velocity, and a similarity solution for Stokes flow at a planar interface (the analytic Huh and Scriven velocity). The relation between the angle and the velocity is determined by performing separate microscopic simulations.

The classical Huh and Scriven solution is only valid for flow over flat walls. In Paper II we use perturbation analysis to extend the solution to flow over curved walls. Paper III presents the parallel finite element solver that is used to perform the numerical experiments presented in this thesis. Finally, the new multiscale model (presented in Paper I) is applied to a relevant microfluidic research problem in Paper IV. For this problem it is very important to have a model that accurately takes the atomistic effects at contact lines into account.

Keywords: Computational fluid dynamics, Two-phase flow, Contact lines

Hanna Holmgren, Department of Information Technology, Numerical Analysis, Box 337, Uppsala University, SE-75105 Uppsala, Sweden.

ISSN 1651-6214
ISBN 978-91-513-0071-9
urn:nbn:se:uu:diva-329059 (http://urn.kb.se/resolve?urn=urn:nbn:se:uu:diva-329059)

List of papers

This thesis is based on the following papers, which are referred to in the text by their Roman numerals.

I H. Holmgren, G. Kreiss. A computational multiscale model for contact line dynamics. *ArXiv e-prints:1709.04917*, 2017. *(Submitted)*

Contributions: The author of this thesis performed the implementation (by modifying the existing two-phase flow solver presented in Paper III) and the numerical experiments. The writing of the manuscript and the ideas were developed in close cooperation between both authors of the paper.

II H. Holmgren, G. Kreiss. A hydrodynamic model of movement of a contact line over a curved wall. *(In revision)*

Contributions: The author of this thesis performed the implementation, calculations and numerical experiments. The ideas and manuscript were developed in close cooperation between both authors.

III M. Kronbichler, A. Diagne, and H. Holmgren. A fast massively parallel two-phase flow solver for microfluidic chip simulation. *The International Journal of High Performance Computing Applications*, 1–22, 2016.

Contributions: The author of this thesis contributed to parts of the writing of the manuscript and to performing some of the simulations. By applying the solver presented in this paper to the problems presented in Paper I–II and Paper IV, the author of this thesis contributed by finding errors and consequently improving parts of the solver. The author of this thesis worked mostly with the level set part of this solver.

IV Z. Ge, H. Holmgren, M. Kronbichler, L. Brandt, and G. Kreiss. Effective slip over partially filled microcavities and its possible failure. Technical Report 2017-019, Department of Information Technology, Uppsala University, September 2017.

Contributions: The author of this thesis performed the simulations in close cooperation with the first author of the paper. Further, the author of the thesis contributed to the writing of the manuscript.

Contents

1 Introduction 7

2 Two-phase flow models 9
2.1 Navier–Stokes equations 9
2.2 Interface representation 10
2.2.1 Level set methods 11

3 Contact lines 14
3.1 The stress singularity 14
3.2 Length scales 15
3.3 Methods for numerical simulation 16

4 Discretization and implementation 19
4.1 Space discretization by the finite element method 19
4.2 Time discretization 20
4.3 Iterative solvers 20
4.4 Implementation 21
4.4.1 Matrix-free implementation 21

5 Summary of papers 23
5.1 Paper I 23
5.2 Paper II 23
5.3 Paper III 24
5.4 Paper IV 24

6 Sammanfattning på svenska 26

Acknowledgements 28

References 30

1. Introduction

Scientific computing involves constructing mathematical models and performing computer simulations with the purpose to answer scientific and engineering questions. These computer simulations complement traditional experiments and theory. The availability of computer simulations has broadened what can be studied without expensive, cumbersome and possibly unethical experiments. One of the largest fields in scientific computing is computational fluid dynamics (CFD), which is used to understand and predict the behavior of fluids.

An important area in CFD is the modeling of two-phase immiscible flows. These are flows involving two different kinds of fluids that do not mix and an interface is separating the two fluids. Examples of two-phase flow phenomena are oil drops in water or ocean waves (where the air is a fluid). Two-phase flow plays an important role in for example process, oil and energy industry. Numerical simulations are fundamental tools and accurate predictions are of growing interest. Challenges when modelling two-phase flows include keeping track of the interface between the two fluids (and possible topological changes) and dealing with surface tension.

This thesis treats the numerical simulation of immiscible incompressible two-phase flows where the fluid-fluid interface is in contact with a solid wall. When the interface is moving over the solid wall, we have a moving contact line problem. The contact line is formed by the intersection of the fluid-fluid interface and the wall. Figure 1.1 illustrates a contact line problem in two space dimensions, where the contact line is reduced to a contact point.

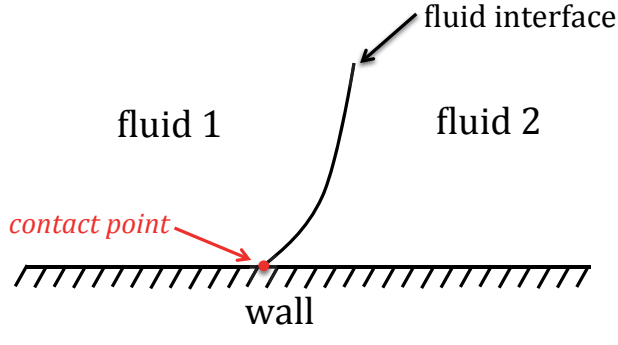

Figure 1.1. Schematic illustration of a contact line problem in two space dimensions, where the contact line is reduced to a contact point.

Moving contact line problems appear in many natural and industrial processes, including any form of droplet spreading on a solid surface, coating flows and displacement flows [14, 58]. Examples from everyday life include raindrops falling on a window and water bugs resting on water surfaces. In many cases the dynamics of the contact line affect the overall behavior of the system [57], which for example is the case for capillary driven flows. Industrial applications where the contact line behavior is important include gas and oil recovery in porous media, lubrication, inkjet printing, biological flows and microfluidics such as micropumps and so called lab-on-a-chip devices [6, 11, 33, 50, 66, 68]. An inkjet device consists of a long ink channel with a tip that ejects liquid drops. With numerical simulations quantities such as the drop size and the ejecting speeds can be predicted [68]. A lab-on-a-chip device can be used to directly diagnose a patient for different diseases by analyzing a single drop of blood, instead of sending a blood sample to a laboratory [64]. These devices involve the flow of different kinds of fluids in miniature channels, and simulations can be used to investigate effects of changing the channel geometry or physical parameters.

Despite their importance, the physics of moving contact lines is poorly understood [14, 11]. Atomistic processes at the contact line come into play, and their influence is difficult to model. The standard Navier–Stokes model is singular when moving contact lines are present. One option is to use models where atomistic scales can be accounted for. Such alternatives include molecular dynamics (MD) or phenomenological based phase field methods (described in Section 2.2). However, it is not realistic to resolve the atomistic processes in a macroscopic domain. Instead, the singularity in the standard Navier–Stokes model can be removed by modifying the model to take phenomena on microscopic length scales into account.

The remainder of this thesis is structured as follows. Chapter 2 gives an overview of different models for the simulation of two-phase flows. This chapter also introduces the level set method, which is used for interface representation in this thesis. Chapter 3 discusses contact line problems and gives a short overview of existing moving contact line models to overcome the difficulty of the singularity. Chapter 4 discusses discretizations and implementations of the equations presented in Chapter 2. Finally Chapter 5 presents a summary of the papers included in this thesis and Chapter 6 gives a summary in Swedish.

2. Two-phase flow models

In this section we consider a domain Ω occupied by two immiscible incompressible fluids separated by an interface Γ, see Figure 2.1. The density and (dynamic) viscosity of the first fluid are denoted by ρ_1 and μ_1 respectively and the domain occupied by this fluid is denoted by Ω_1, and similarly for the second fluid.

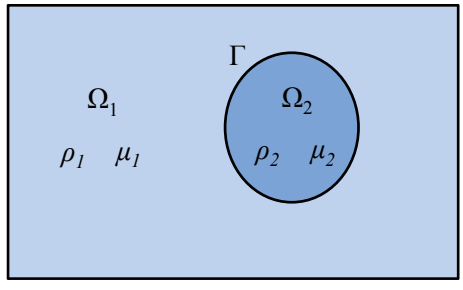

Figure 2.1. Model domain Ω. Fluid 1 with density ρ_1 and viscosity μ_1 occupies Ω_1 and fluid 2 with density ρ_2 and viscosity μ_2 occupies Ω_2. The separating interface is denoted by Γ.

2.1 Navier–Stokes equations

The motion of each fluid in Figure 2.1 is given by the incompressible Navier–Stokes equations for the fluid velocity $\mathbf{u}$ and pressure p

$$\rho\left(\frac{\partial \mathbf{u}}{\partial t}+\mathbf{u}\cdot\nabla\mathbf{u}\right)=-\nabla p+\nabla\cdot(2\mu\nabla^{\mathrm{s}}\mathbf{u})+\mathbf{f}, \tag{2.1}$$

$$\nabla\cdot\mathbf{u}=0. \tag{2.2}$$

The rank-2 tensor $\nabla^{\mathrm{s}}\mathbf{u}=\frac{1}{2}(\nabla\mathbf{u}+\nabla\mathbf{u}^{T})$ denotes the rate of deformation and the term $\mathbf{f}$ represents external forces.

At the interface between the two immiscible fluids, surface tension forces act in order to drive the interface into a state of minimum surface energy. Coupling conditions at the interface Γ are needed

$$[\![\mathbf{u}]\!]_{\Gamma}=\mathbf{0} \quad \text{- continuity of velocity,} \tag{2.3}$$

$$[\![2\mu\nabla^{\mathrm{s}}\mathbf{u}\cdot\mathbf{n}]\!]_{\Gamma}\cdot\mathbf{t}=0 \quad \text{- continuity of shear stress,} \tag{2.4}$$

$$[\![-p\mathbf{n}+2\mu\nabla^{\mathrm{s}}\mathbf{u}\cdot\mathbf{n}]\!]_{\Gamma}=\sigma\kappa\mathbf{n} \quad \text{- balance of normal stress and surface tension} \tag{2.5}$$

where $[\![\mathbf{u}]\!]_\Gamma$ represents the jump of the quantity $\mathbf{u}$ from Ω_1 to Ω_2, $\mathbf{n}$ and $\mathbf{t}$ denote normal and tangential directions to the interface Γ, σ controls the magnitude of surface tension and κ is the interface curvature.

Instead of solving equations (2.1)–(2.2) and the coupling conditions (2.3)–(2.5) twice, once for each fluid, the Navier–Stokes equations can be reformulated to be valid in the whole domain Ω. In this formulation the effect of surface tension is modeled by adding a forcing to the momentum equation (2.1)

$$\mathbf{f}_{st} = \sigma\kappa\mathbf{n}\delta_\Gamma, \tag{2.6}$$

where the delta function δ_Γ localizes the force to the interface Γ. For example, δ_Γ localizes a smooth function v by

$$\int_\Omega \delta_\Gamma v \, d\Omega = \int_\Gamma v \, d\Gamma. \tag{2.7}$$

The Navier–Stokes equations are completed by a divergence-free initial condition for the fluid velocity $\mathbf{u}(\cdot, 0)$. At a fixed solid wall a no-slip boundary condition that prescribes a zero fluid velocity is often used.

A so-called creeping flow occurs if the viscous effects dominate the convection. The convection term and the time derivative on the left hand side of the momentum equation (2.1) can then be neglected and the non-linear Navier–Stokes equations reduce to the linear Stokes equations (under the assumption of linear viscosity).

2.2 Interface representation

Two-phase flow models require a method for tracking and evolving the fluid interface in time. Several interface representation techniques have been proposed during the last decades. A historical overview of models and methods is given for example in [62].

The two main classes of two-phase flow models are interface tracking and interface capturing methods. Interface tracking methods use an explicit representation of the interface. Examples are front-tracking methods [22, 63, 44] where a set of marker points are used to explicitly represent the interface. The interface is evolved by advecting each marker point by the local fluid velocity. The fluid velocity is often obtained by solving the Navier–Stokes equations on an Eulerian grid and the velocities at the marker points are then obtained by interpolation. After deformation of the interface the marker points will not be evenly distributed and in some parts there may be a clustering of markers. Redistribution of the markers is therefore necessary to retain accurate interface representations. Further, tracking methods suffer from unphysical volume changes of the two fluid phases. However, a good accuracy of the method is possible since a large number of marker points can be used.

In interface capturing methods the interface is implicitly represented by a higher dimensional function (compared to the interface). Interface capturing methods therefore provide a natural mechanism for handling topological changes such as merging or breaking of interfaces. In the volume-of-fluid (VOF) method [25], the so-called fluid function keeps track of the volume fraction of each fluid in each grid cell. The fluid function takes a value between zero and one in each cell, depending on the volume fraction of the corresponding fluid. The interface is usually advected by increasing or decreasing the volume fraction in each cell according to the velocity field and the composition of neighboring cells. A reconstruction of the interface from the volume fractions is required for the evaluation of surface tension forces. These reconstruction techniques use approximations by for example piecewise constants [25], piecewise linear functions [49] or splines [20]. The volume-of-fluid methods conserve mass well. However, the reconstruction of the interface makes them more complicated to implement compared to for example front tracking methods.

Other examples of interface capturing methods are level set [43, 60] and phase field methods [28]. These methods use continuous functions to represent the interface (as opposed to the volume-of-fluid method where a discrete representation is used). In the papers in this thesis different versions of the level set method are used for interface dynamics, and this method is therefore presented in more detail in the next subsection.

In phase field methods the interface is modeled as having a finite thickness, i.e. a diffuse interface. The smoothed region between the different fluids is described in a thermodynamically consistent way; the idea comes from the van der Waals hypothesis that immiscible fluids do mix at a molecular level. However the modeled thickness of the smoothed region is usually much larger than it is in real systems. To update the so-called phase function, which identifies the different fluids, a continuum advection-diffusion equation is used. This equation originates from the Cahn–Hilliard equation [8], which models the seeking of minimal energy of the physical system. A drawback with the phase field method is that a high resolution is required since the propagation and interface properties are sensitive to the dynamics in the smoothed region, [67].

2.2.1 Level set methods

Level set methods use a continuous level set function to represent the interface. The level set function $\phi(\mathbf{x})$ is defined on the whole domain Ω (Figure 2.1), and the fluid interface Γ is defined as the zero level set of ϕ. In the standard level set method (used in Paper II) the level set function ϕ is a signed distance

function [52]

$$\phi(\mathbf{x}) = \begin{cases} \text{dist}(\mathbf{x},\Gamma) & \text{in the first fluid,} \\ -\text{dist}(\mathbf{x},\Gamma) & \text{in the second fluid.} \end{cases} \tag{2.8}$$

The expression $\text{dist}(\mathbf{x},\Gamma)$ represents the shortest distance from the position $\mathbf{x}$ to the interface Γ. Figure 2.2 shows the signed distance function ϕ for the case of a two-dimensional circular fluid interface. The black contour illustrates the zero level set, i.e. the interface.

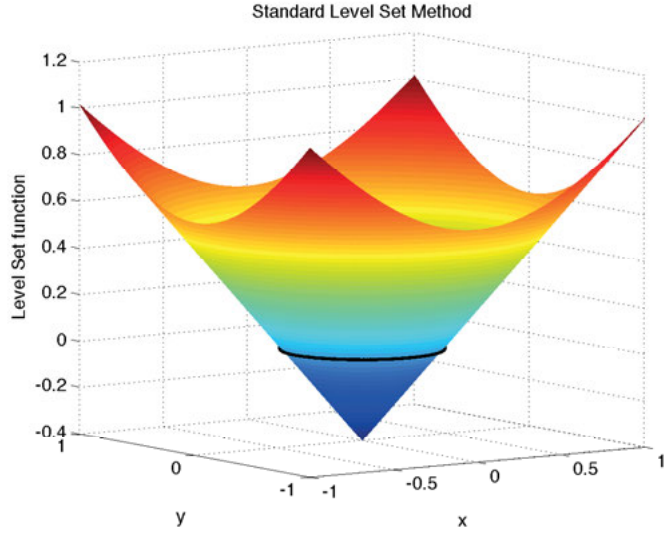

Figure 2.2. The signed distance function (in color) to the circular interface (the black contour).

The interface is evolved by advection of the level set function with the local fluid velocity according to a Hamilton–Jacobi equation

$$\frac{\partial \phi}{\partial t} + \mathbf{u} \cdot \nabla \phi = 0. \tag{2.9}$$

For evaluation of the surface tension force (2.6) the calculation of normal vectors and curvature of the interface is required. The level set methods allow for straight-forward calculations by

$$\mathbf{n} = \frac{\nabla \phi}{|\nabla \phi|}$$
$$\kappa = -\nabla \cdot \mathbf{n}.$$

The level set function will lose its signed distance property during the simulation due to discretization errors and non-uniform velocity fields. To smooth

the level set function and prevent the formation of large gradients, ϕ has to be restored regularly to take the form of a signed distance function. When ϕ is a signed distance function it has the property $|\nabla\phi| = 1$. The standard way to restore, or reinitialize, the level set function is to solve the following equation to steady state [60]

$$\frac{\partial\phi}{\partial\tau} + \text{sign}(\phi_0)(|\nabla\phi| - 1) = 0, \tag{2.10}$$

where ϕ_0 is the level set function before reinitialization and τ is a pseudo time. A regularized sign-function that smoothly changes sign from $+1$ in the first fluid to -1 in the second fluid is often used.

The standard level set method often suffers from unphysical volume changes. Several methods exist to improve mass conservation. One example is the so-called conservative level set method [41, 42] which is used in Paper I and Paper III–IV. This method uses a level set function that smoothly switches value from $+1$ to -1 in a small transition region of size ε around the interface, instead of a signed distance function. Further, the reinitialization is posed as a conservation law where $\int_\Omega \phi \, d\mathbf{x}$ is preserved by solving the following equation to steady state

$$\frac{\partial\phi}{\partial\tau} + \nabla\cdot(\mathbf{n}(1-\phi^2)) - \nabla\cdot(\mathbf{n}\varepsilon\nabla\phi\cdot\mathbf{n}) = 0. \tag{2.11}$$

Another example is hybrid methods, such as the combined level set–VOF method [59].

3. Contact lines

When an interface separating two immiscible fluids is in contact with a solid wall, a contact line is formed at the intersection of the interface and the solid. In two space dimensions the contact line is reduced to a contact point (as illustrated in Figure 1.1). The standard Navier–Stokes equations together with the conventional no-slip boundary condition predicts a singularity in the shear stresses at the contact line [27, 15]. In fact, molecular dynamics simulations show that there must be some fluid-wall slip in the region close to the contact line (on an atomistic length scale) [31, 61]. Therefore, microscopic length scales must be introduced into the problem [17]. In the case of capillary driven flows for example, it has been observed that the microscopic contact line dynamics has a large impact on the overall macroscopic flow. However, the physics behind this interaction is not completely understood [6, 27, 57].

The fine-scale nature of the contact line dynamics represents a significant numerical difficulty, as it is several orders of magnitude smaller than the global scale in many important applications [35]. Molecular dynamics simulations are limited to very small systems of a few tens of nanometers and a few nanoseconds [36]. Consequently, simulations of moving contact line problems of typical sizes of millimeters can not be performed by resolving all the length scales.

This chapter first discusses the physics behind dynamic contact lines and then gives an overview of different existing models to perform computer simulations.

3.1 The stress singularity

For equilibrium situations, the physics of the contact line has been understood for a long time [11]. The static contact angle θ_s, which is formed between the fluid interface and the solid, depends on the surface tension coefficient at the interface σ and the surface tension coefficients between the solid and the two fluids σ_1 and σ_2 respectively. Minimizing the total surface energy leads to Young's relation for the static contact angle θ_s

$$\sigma_2 - \sigma_1 = \sigma \cos\theta_s. \tag{3.1}$$

For moving contact lines, the situation is more complicated. The dynamic contact angle depends in a complicated way on the local dynamics at the moving contact line [7]. In the paper by Huh and Scriven [27] it is argued that

the situation is in essence described by a corner flow with no intrinsic length scale. There, the system is modeled using the two-dimensional Stokes equations with the no-slip boundary condition at the solid surface [65]. An analytic solution for the flow in a wedge is derived assuming a perfectly planar fluid interface [57]. It is observed that in the analytic solution stresses and viscous dissipation increase without bound when the contact line is approached [65]. This singularity still remains when the full Navier-Stokes equations are used [65]. Further, Dussan and Davis show that if the no-slip boundary condition is applied and the contact line moves, then necessarily the stress tensor must have a singularity [65].

3.2 Length scales

The physics at different length scales is illustrated by the successive close-ups near the contact line in Figure 3.1. In the macroscopic region, of typical length scales $L > 10^{-7}$ m , the flow and the interface shape may be influenced by several different physical phenomena such as capillarity, gravity etc. When capillarity is important, the large scale flow is mainly governed by either inertia and surface tension, or by viscosity and surface tension. Flow situations where inertia and surface tension are dominating are characterized by low Ohnesorge numbers $\mathrm{Oh} = \frac{\mu}{\sqrt{\rho\sigma L}} = \frac{\sqrt{\mathrm{We}}}{\mathrm{Re}} = \sqrt{\frac{\mathrm{Ca}}{\mathrm{Re}}}$, where μ is the fluid viscosity, σ is surface tension, ρ is the fluid density and L is a characteristic length scale [12]. The length scale L could for example be the physical width of a channel, or the cross section of a droplet or a cavity. Further, the Weber number, We, relates inertia to surface tension, the Reynolds number, Re, relates inertia to viscous forces and the Capillary number, Ca, relates viscous forces to surface tension.

At smaller scales, illustrated by the intermediate region in Figure 3.1, the flow is governed by a viscocapillary balance [54, 39]. This balance is characterized by the capillary number $\mathrm{Ca} = \frac{\mu U}{\sigma}$, where U is a characteristic velocity. As mentioned above, the capillary number represents the relative effect of viscous forces versus surface tension acting across an interface. At a viscocapillary balance $Ca \sim 1$. At this scale the interface shape is influenced by viscous effects and the interface will be strongly curved close to the contact line [29]. Extrapolating the outer interface shape toward the contact line leads to an apparent macroscopic contact angle θ, see Figure 3.1.

At the molecular length scale of $L < 10^{-9}$ m, the blue region in Figure 3.1, the conventional hydrodynamics break down and other models are necessary [54, 39]. More details on the physics of dynamic contact lines are given in for example the review papers [6, 54, 57].

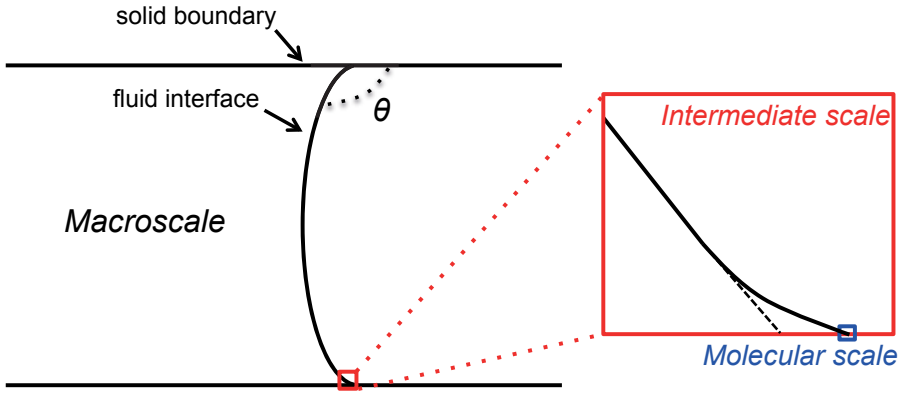

Figure 3.1. Schematic illustration of the different length scales.

3.3 Methods for numerical simulation

Different contact line models are reviewed in for example [57, 39, 36]. One of the best documented methods to overcome the stress singularity at the moving contact line is to replace the no-slip condition with a Navier slip condition [58, 54, 36]

$$\mathbf{u}_{\text{slip}} = \lambda \mathbf{n} \cdot (\nabla \mathbf{u} + (\nabla \mathbf{u})^T), \tag{3.2}$$

introducing a related slip length parameter λ (here $\mathbf{n}$ is the normal vector of the boundary). However, unrealistically large slip length values are necessary for most of these simulations due to grid refinement limitations [36]. Additionally, when capillarity is important for the large scale flow, contact line dynamics also need to be accounted for. The slip condition then needs to be combined with a prescribed dynamic contact angle or velocity [57, 58]. The simplest approach is to impose a constant angle corresponding to the static angle θ_s [48, 30, 37, 56, 2]. For cases when the large scale flow is governed mainly by inertia and surface tension (i.e. low Ohnesorge numbers), the dynamic angle is close to the static angle [12] and static models can perform rather well [36].

When the large scale motion is mainly governed by viscosity and surface tension (i.e. high Ohnesorge number in capillary driven flows), the evolution is directly dependent on the contact line velocity, and the dynamic contact angle differs from the static one [57, 12]. Instead, large scale simulations need some sort of sub-grid modelling to account for the microscopic effects. A common approach is to prescribe an apparent contact angle according to an empirical law [6] or hydrodynamics theories [9, 10, 26, 40]. In [58, 13, 66, 3, 55] for example the Cox theory [9] is used to relate the apparent contact angle to the microscopic angle and contact line speed by

$$g(\theta_L) = g(\theta_s) + \text{Ca} \log\left(\frac{L}{\lambda}\right). \tag{3.3}$$

Here λ is the slip length and L is the macroscopic cut-off length scale imposed by the grid resolution where the angle θ_L is measured [36]. The explicit expressions for $g(\theta)$ are given in for example [58]. The Cox relation is either directly applied [58, 13, 55] or by using an adjustable parameter that needs to be empirically determined from experiments [66, 3]. Further, the Cox theory is based on the special case of lubrication theory, and the appropriate dynamic contact angle will depend on the scale on which matching between outer and inner scales occurs [6]. Also, even though the contact line dynamics can be prescribed by relating the apparent contact angle to the microscopic angle and/or contact line speed (by for example equation (3.3)), it is not clear how this condition should be imposed at the macroscopic level. Often ad-hoc regularizations are used to apply velocity boundary conditions along the whole solid wall. In [53] for example, a slip profile that decays exponentially to no-slip far from the contact line is implemented.

A different approach is found in the phase field method, described in Section 2.2, where molecular processes at the interface between fluids and at the contact line are modeled by diffusion [28]. In this model, contact line dynamics is handled by a boundary condition relating the surface energy to the contact angle via Young's relation. With this approach there is no singularity of the stress when the no-slip boundary condition is used for velocity. However, the diffusion processes need to be modeled at physically relevant length scales, which means tens to hundreds of nanometers [67]. As argued in Section 2.2, this becomes very computationally demanding, and therefore unphysically large diffusion parameters are often used.

Another option is to use a multiscale approach where different physical descriptions at different length scales are coupled by for example using the heterogeneous multiscale method [1, 16, 46]. The micromodel is usually based on molecular dynamics [61, 45, 47]. However, these multiscale models have only been applied to two-phase systems in Couette or Poisseuille flows where the densities and viscosities are assumed to be the same in the two fluids.

Paper I presents a new multiscale method where a conventional macroscale solver is coupled to the local phase field solver in [35]. In [35] phase field computations determine a quasi-steady state in a contact point region for a particular apparent contact angle. The relation between the angle and the corresponding contact point velocity characterizes the local dynamics in the contact point region, as discussed in [54]. A direct coupling between the two models would require the macro resolution to match the micro resolution at the interface between the two domains. Due to the scale separation such a matching would be computationally challenging. In Paper I we take a different approach where we use the analytic Huh and Scriven solution to bridge the gap between the scales of the micro region and those of the global features of the flow. Based on the Huh and Scriven similarity solution we formulate boundary conditions for the Navier–Stokes system at an artificial boundary,

which is placed at a distance from the contact point such that the features of the flow can be resolved at the global scale.

4. Discretization and implementation

Discrete approximations of the solution to the Navier–Stokes equations (2.1)–(2.2) and to the equation for interface advection (2.9) are required for macroscopic numerical simulation of moving contact line problems. Both spatial and temporal discretizations are necessary. The most popular methods for discretization in space are the finite volume method, the finite difference method and the finite element method. In this thesis the finite element method is used.

4.1 Space discretization by the finite element method

The first step in the finite element approximation is to rewrite the equations on variational form. The variational form of the Navier–Stokes equations (2.1)–(2.2) reads: find $\mathbf{u} \in V_{\mathbf{u}}$ and $p \in V_p$ such that

$$\left(\mathbf{v}, \rho\left(\frac{\partial \mathbf{u}}{\partial t} + \mathbf{u}\cdot\nabla\mathbf{u}\right)\right)_\Omega = (\nabla\cdot\mathbf{v}, p)_\Omega - (\nabla^{\mathrm{s}}\mathbf{v}, 2\mu\nabla^{\mathrm{s}}\mathbf{u})_\Omega + (\mathbf{v}, \mathbf{f})_\Omega \tag{4.1}$$

$$(q, \nabla\cdot\mathbf{u})_\Omega = 0 \tag{4.2}$$

for all test functions $\mathbf{v} \in V_{\mathbf{u}}$ and $q \in V_p$. Here $(\cdot,\cdot)_\Omega$ is the standard L_2 inner product on Ω and $V_p = L_2(\Omega)$. $V_{\mathbf{u}}$ is the space of all square integrable vector-valued functions on the domain Ω with integrable first derivatives that satisfy the boundary conditions, i.e. $V_{\mathbf{u}} = \{\mathbf{u} \in H^1(\Omega); \mathbf{u} = 0 \text{ on } \partial\Omega\}$. For simplicity, only the theory for no-slip boundary conditions is presented here, for other types of conditions see [23].

The variational formulation for the level set equation (2.9) reads: Find $\phi \in V_\phi = H^1(\Omega)$ such that

$$\left(\eta, \frac{\partial \phi}{\partial t} + \mathbf{u}\cdot\nabla\phi\right)_\Omega = 0 \tag{4.3}$$

for all test functions $\eta \in V_\phi$.

In the next step, the solution function spaces $V_{\mathbf{u}}, V_p$ and V_ϕ are replaced by finite-dimensional discrete subspaces $V_{\mathbf{u}}^h, V_p^h$ and V_ϕ^h. In the work presented here, the computational domain is decomposed into quadrilateral elements of size h. Further, the basis functions that span $V_{\mathbf{u}}^h$ are piecewise quadratic polynomials and the functions that span V_p^h and V_ϕ^h are piecewise linear polynomials. The basis functions are nonzero in exactly one node of the domain, and

zero at all other nodes. The finite element method for the Navier–Stokes equations does not allow for arbitrary pairings of basis functions for the velocity and pressure spaces due to the Babuška–Brezzi (inf–sup) condition [21] (unless stabilization techniques are applied). This is the reason for the difference in the degrees of the polynomials that span the discrete velocity and pressure spaces. The discrete approximations $\mathbf{u}^h$, p^h and ϕ^h are on the form

$$\mathbf{u}^h = \sum_{j=1}^{N_u} U_j \mathbf{v}_j^h, \quad p^h = \sum_{j=1}^{N_p} P_j q_j^h, \quad \phi^h = \sum_{j=1}^{N_\phi} \Phi_j \eta_j^h. \tag{4.4}$$

where the coefficients U_j, P_j and Φ_j are to be determined and the functions $\mathbf{v}_j^h$, q_j^h and η_j^h span the spaces $V_{\mathbf{u}}^h$, V_p^h and V_ϕ^h respectively. Now, the finite element approximation of the Navier–Stokes equations is to find the discrete velocity $\mathbf{u}^h \in V_{\mathbf{u}}^h$ and pressure $p^h \in V_p^h$ such that a variational formulation of the form (4.1)–(4.2) is fulfilled for all test functions $\mathbf{v}^h \in V_{\mathbf{u}}^h$ and $q^h \in V_p^h$. Similarly, the level set equation is discretized by finding the discrete level set function $\phi^h \in V_\phi^h$ such that a variational formulation of the form (4.3) is fulfilled for all test functions $\eta_h \in V_\phi^h$.

4.2 Time discretization

In this thesis the Navier–Stokes equation and the level set equation are both discretized in time using the implicit Backward Differentiation Formula of second order (BDF-2). However, to avoid an expensive coupling between the Navier–Stokes part and the level set part (via the variables $\mathbf{u}$ and ϕ), an explicit splitting scheme between the two equations is introduced. At each time step n, an estimate of the level set function is extrapolated from the values at time steps $n-1$ and $n-2$. This estimate is used to evaluate the surface tension force. Then, the BDF-2 time step for the Navier–Stokes equations is performed. Finally, the level set function is propagated in time using the velocity $\mathbf{u}^n$ obtained from the Navier–Stokes step, also using the BDF-2 scheme. The splitting corresponds to an explicit treatment of surface tension and therefore imposes a restriction on the time step, see [19] for details.

4.3 Iterative solvers

The combination of the finite element method and implicit time discretization schemes for the solution of the Navier–Stokes equations results in a system of equations on saddle point form. Finding solutions to these problems is challenging. In this thesis the saddle point system is solved by an iterative GMRES solver [51]. For preconditioning, a block-triangular operator constructed using the so called Schur complement of the block system is applied from the

right [18]. The resulting linear system of equations from discretizing the level set equation is solved using a BiCGStab solver [51] due to non-symmetry. For more details about the linear solvers we refer to Paper III.

Instead of solving the Navier–Stokes equations using implicit time discretization, there are explicit methods where the saddle-point linear system is avoided. In these so-called fractional step schemes the momentum equation (2.1) is first solved using a pressure that is extrapolated from old time levels. The resulting velocity is in general not divergence free. Because of this a pressure Poisson equation with forcing according to the divergence of the intermediate step velocity is solved to correct the velocity. The two subproblems result in systems that are considered to be of an easier structure than a saddle point problem. However, imposing boundary conditions is not straightforward and many naive implementations suffer from inconsistent approximations close to boundaries [24]. Further, in two-phase flow simulations the implementation of the case when the two fluids have different density is not straightforward and the Poisson solvers are less efficient.

4.4 Implementation

In this thesis, the implementation is done using the existing two-phase flow solver described in Paper III with suitable modifications to account for moving contact lines. Additionally, the order in which the equations are solved in each time step is changed (so that the Navier–Stokes equations are solved before the interface is advected, as described in previous section). The solver is implemented in the C++ based finite element open source library deal.ii [4, 5].

4.4.1 Matrix-free implementation

Most of the iterative solvers spend the bulk of the computing time in matrix-vector products. Implementations of these algorithms on today's processors, access to main memory has become a bottleneck: more time is spent reading data from memory than actually performing the floating point operations. A possible way to decrease the run-time is to substitute the process of reading matrix elements from memory by re-computing them instead [32, 34]. This idea builds on the fact that for iterative solvers the system matrix is never needed explicitly, but rather the effect of multiplication with a vector. The standard process (where the global matrix is stored in memory) is to first assemble the global system matrix by adding small local element-matrices, and then multiply the resulting global system matrix with a vector. With the modified matrix-free method one instead performs a lot of small local matrix-vector multiplications and then adds the local results to the resulting global vector,

i.e. the global resulting vector is assembled directly without storing the global matrix.

The matrix-free approach results in a large number of small and dense matrix-vector products. So, one needs to optimize the details of the local matrix-vector operations to gain performance [38]. In Paper III the matrix-free method from [32, 34] is used for matrix-vector products. This method is based on fast cellwise integration using the fact that the basis functions for quadrilateral and hexahedral elements can be expressed as tensor products of d one dimensional basis functions. More details on the matrix-free method and how the local operations are optimized can be found in the aforementioned references [32, 34] and also in [38]. The method in [32, 34] enables matrix-free matrix-vector products that are up to an order of magnitude faster on piecewise quadratic elements.

5. Summary of papers

5.1 Paper I

H. Holmgren, G. Kreiss. A computational multiscale model for contact line dynamics. *ArXiv e-prints:1709.04917*, 2017. *(Submitted)*

Paper I presents a new multiscale model for numerical simulation of flow of two immiscible and incompressible fluids in the presence of moving contact points. More specifically, the paper presents a new boundary methodology based on combining a relation between apparent contact angle and contact point velocity, and the similarity solution for Stokes flow at a planar interface (i.e. the analytic Huh and Scriven velocity from [27]). The relation between the angle and velocity is determined by performing micro simulations using the phase field model. These simulations use physically relevant phase field parameters for molecular diffusion and interface thickness. The methodology is used to formulate a new boundary condition for the velocity. Numerical results illustrate the usefulness.

Contributions
The author of this thesis performed the implementation (by modifying the existing two-phase flow solver presented in Paper III) and the numerical experiments. The writing of the manuscript and the ideas were developed in close cooperation between both authors of the paper.

5.2 Paper II

H. Holmgren, G. Kreiss. A hydrodynamic model of movement of a contact line over a curved wall. *(In revision)*

The multiscale model presented in Paper I uses the analytic Huh and Scriven velocity from [27], which is only valid for flow over a flat wall. In Paper II a perturbation analysis of the classical Huh and Scriven solution is performed to obtain a two-dimensional hydrodynamic model for the velocity field at a contact point moving over a curved wall (instead of a flat wall). Also, the paper presents the first steps in developing the multiscale model from Paper I. Paper II presents a first idea for how the hydrodynamic solution could be used to prescribe macroscopic Dirichlet boundary conditions for the velocity in the vicinity of a moving contact point. Simulations demonstrate that the velocity field based on the non-singular boundary conditions is capable of accurately advecting the contact point.

Contributions
The author of this thesis performed the implementation, calculations and numerical experiments. The ideas and manuscript were developed in close cooperation between both authors.

5.3 Paper III

M. Kronbichler, A. Diagne, and H. Holmgren. A fast massively parallel two-phase flow solver for microfluidic chip simulation. *The International Journal of High Performance Computing Applications*, 1–22, 2016.

Paper III presents a parallel finite element solver of incompressible two-phase flow. The solver is optimized for large-scale simulations of three-dimensional dynamics. The paper presents results for an example of a large-scale application in the form of high-throughput microfluidic separation devices. The two-phase implementation relies on a conservative level set formulation for representing the fluid-fluid interface and uses adaptive mesh refinement. An implicit time stepping with efficient block solvers for the incompressible Navier–Stokes equations is presented. A matrix-free implementation is used that reduces the solution time for the Navier–Stokes system by a factor of approximately three compared to the best matrix-based algorithms. Scalability of the chosen algorithms up to 32,768 cores and a billion degrees of freedom is shown.

Contributions
The author of this thesis contributed to parts of the writing of the manuscript and to performing some of the simulations. By applying the solver presented in this paper to the problems presented in Paper I–II and Paper IV, the author of this thesis contributed by finding errors and consequently improving parts of the solver. The author of this thesis worked mostly with the level set part of this solver.

5.4 Paper IV

Z. Ge, H. Holmgren, M. Kronbichler, L. Brandt, and G. Kreiss. Effective slip over partially filled microcavities and its possible failure. Technical Report 2017-019, Department of Information Technology, Uppsala University, September 2017.

In Paper IV the multiscale model for contact line dynamics presented in Paper I is applied to a relevant microfluidic research problem: the static drag reduction over a lubricant-infused surface is studied by studying an array of

two-dimensional transverse grooves partially filled with a second immiscible fluid. Microscale roughness on an otherwise smooth hydrophobic surface can significantly reduce the resistance to an external liquid flow. Numerical simulations using the method from Paper I are used to probe the static drag reduction property and the dynamic wetting behavior. The dependence of the effective slip (i.e. the drag reduction) is studied by varying the viscosity ratios, capillary numbers, the static contact angle and the filling rate of the cavity (meaning the amount of lubricant fluid). An increase of the effective slip with the cavity filling is observed and a potentially new failure mode is identified.

Contributions
The author of this thesis performed the simulations in close cooperation with the first author of the paper. Further, the author of the thesis contributed to the writing of the manuscript.

6. Sammanfattning på svenska

Beräkningsvetenskap innebär att konstruera matematiska modeller och utföra datorsimuleringar för att försöka svara på vetenskapliga och tekniska frågeställningar. Datorsimuleringar kompletterar traditionella experiment och teorier. Möjligheten till datorsimuleringar har gjort att man kan undersöka sådant som till exempel varit för dyrt, avancerat eller oetiskt för att kunna utföra traditionella experiment. Ett av de största områdena inom beräkningsvetenskap är strömningsmekaniska beräkningar (CFD). Dessa används för att förstå och förutsäga beteendet hos vätskor och gaser, så kallade fluider.

Ett viktigt område inom CFD är modellering av system som involverar två olika sorters fluider, så kallade tvåfasflöden. Denna avhandling fokuserar på tvåfasflöden där de två vätskorna eller gaserna är icke blandbara, d.v.s. ett gränsskikt bildas mellan de två fluiderna. Exempel på sådana tvåfasflöden är oljedroppar i vatten och havsvågor, där luften också räknas som en fluid. Tvåfasflöden förekommer till exempel i energi-, olje- och processindustrier där numeriska simuleringar är grundläggande verktyg för att kunna göra noggranna förutsägelser. Utmaningar och svårigheter vid modellering av tvåfasflöden innefattar bland annat att kunna följa gränsskiktets rörelse samt att behandla ytspänningen mellan de två fluiderna.

Denna avhandling behandlar numeriska simuleringar av icke blandbara tvåfasflöden där gränsskiktet mellan de två fluiderna är i kontakt med en vägg eller annat fast material. När gränsskiktet rör sig över det fasta materialet uppstår ett så kallat dynamiskt kontaktlinjeproblem. Kontaktlinjen bildas där gränsskiktet mellan de två fluiderna möter det fasta materialet. Figur 1.1 visar en schematisk bild på ett kontaktlinjeproblem i två dimensioner, där kontaktlinjen reduceras till en kontaktpunkt.

Dynamiska kontaktlinjeproblem förekommer i många naturliga och industriella processer. Exempel från vardagen inkluderar regndroppar som faller på ett fönster eller ett löv, vätska som sugs upp i ett sugrör och skräddare (insekter) som vilar på vattenytan i en sjö. I många fall påverkar beteendet hos kontaktpunkten det övergripande beteendet hos hela systemet [57], vilket till exempel är fallet för system där kapillärkrafter driver flödet. Industriella processer där kontaktlinjedynamiken har stor inverkan på resten av flödet inkluderar till exempel gas- och oljeflöden i porösa medier, smörjning, flödet av bläck i skrivare, biologiska flöden och mikrofluidik [11, 66, 6, 50, 68, 33]. Mikrofluidik förekommer till exempel i så kallade mikropumpar eller lab-on-a-chips. Ett lab-on-a-chip kan användas för snabb diagnostisering av olika sjukdomar eller allergier genom att analysera en enda bloddroppe istället för att skicka ett

helt blodprov till ett laboratorium [64]. Dessa chip involverar flöden av olika sorters vätskor i miniatyrkanaler och datorsimuleringar kan användas för att undersöka effekten av att till exempel ändra kanalstorlekarna eller andra fysiska parametrar. I en bläckstråleskrivare flödar bläcket först i en lång kanal för att sedan matas ut i små droppar i slutet av kanalen. Med datorsimuleringar kan man till exempel undersöka droppstorlekens och utmatningshastighetens inverkan på resultatet [68].

Trots att dynamiska kontaktlinjeproblem är så pass vanliga har man fortfarande inte helt utrett de bakomliggande fysikaliska processerna [14, 11]. Man vet dock att atomistiska processer vid kontaktlinjen har en inverkan, men dessa är svåra att modellera. Standardmetoden för att beskriva flöden av vätskor innebär bland annat att lösa Navier–Stokes ekvationer. Om man försöker använda denna modell för flöden där dynamiska kontaktlinjer förekommer uppstår en singularitet i modellen. Ett alternativ är att istället använda modeller där atomistiska längdskalor inkluderas. Exempel på sådana modeller är molekyldynamiska simuleringar eller så kallade phase field-metoder. Det är dock bara möjligt att använda dessa modeller för flödet precis intill kontaktlinjen, inte för hela system där kontaktlinjer förekommer, eftersom längdskalorna är så pass olika. Ett annat alternativ innebär att modifiera standardmodellen så att den tar hänsyn till de atomistiska processerna, utan att faktiskt utföra detaljerade simuleringar på de längdskalorna.

I Manuskript I presenteras en ny modell för simulering av dynamiska kontaktlinjeproblem. I den nya modellen tas de atomistiska processerna vid kontaktlinjen till hänsyn via speciella randvillkor. Dessa randvillkor använder resultat från lokala phase field-simuleringar som utförs i området precis vid kontaktlinjen. Randvillkoren beror även på teoretiska uttryck som beskriver flödet i närheten av kontaktlinjer (men ej exakt vid kontaktlinjen, och ej heller långt från kontaktlinjen).

I Manuskript II utvidgas de teoretiska uttrycken så att de även gäller för flöden över fasta objekt som inte nödvändigtvis har en plan yta. Manuskript III presenterar den programvara som har använts för att utföra datorsimuleringar (i Manuskript I–II och IV). Avslutningsvis används den nya metoden (från Manuskript I) för att utföra datorsimuleringar där syftet är att undersöka en vetenskaplig frågeställning gällande ett specifikt mikrofluidiskt system. För detta system är det viktigt att använda en noggrann modell som inkluderar atomistiska effekter vid kontaktlinjen.

Acknowledgements

First of all, I would like to thank my main advisor, Gunilla Kreiss. Thank you for your guidance, I have learned a lot from you and your broad knowledge of numerical analysis. Also, thanks for many interesting discussions, and for the company when learning more about the physics of contact lines. Secondly, I want to thank my co-author and informal second advisor Martin Kronbichler. Thank you for sharing all your knowledge, for answering all my questions during these years (probably quite a few if you would count them) and for all the discussions we had that often were important for me to make progress in my research projects. Also, thanks to my other collaborators and co-authors, Ababacar Diagne, Zhouyang Ge and Luca Brandt.

Simon, thank you for our collaboration writing the code for the reinitializer; this was one of the most fun research projects during my PhD-studies. I learned a lot about programming, and you had the patience to answer all my questions until I understood. I really enjoy collaborating closely with someone, and it was very nice to be able to do this with you. Also, thanks for the help with a lot of other things; you almost always have an answer to my questions no matter if they are programming, research, teaching or course related!

I would like to thank all the people who helped proofreading this comprehensive summary, amongst others Martin Almquist, Simon Sticko and Fredrik Hellman. Slobodan Milovanović, thank you for the help with editing the front page photo. Furthermore, I want to express my gratitude for the good leadership and management skills of Lina von Sydow. Also, thanks goes to Kronofogden.

To all my great friends at TDB (present and former): I am privileged to have met you! Simon and Slobodan, our offie is the best. I really enjoyed your company and our little office-family. Thanks for your support during these years. Also, special thanks to Josefin Ahlkrona, Lina Meinecke, Martin Almquist, Fredrik Hellman, Martin Tillenius and Siyang Wang for being great friends and support.

To all my friends outside TDB, thank you! Special thanks to Anna Hellbom for your great friendship and never ending supporting words. Kristoffer Wahlberg, thank you for all your unconditional support. Thank you for surviving these years and for still being my *sambo*. Last but definitely not least, a big thanks to my great family: Mamma, pappa, Johan, David, Stina, Felix och Viggo, you are the best family!

This work was supported by the Swedish Research Council 621-2012-2360. The computations were partly performed on resources provided by the Uppsala Multidisciplinary Center for Advanced Computational Science (Uppmax) at Uppsala University and the Leibniz Supercomputing Center in Munich. Funding for travels has been gratefully received from Anna-Maria Lundins stipendiefond, Liljevalch resestipensium and Knut och Alice Wallenbergs stiftelse.

References

[1] A. Abdulle, E. Weinan, B. Engquist, and E. Vanden-Eijnden. The heterogeneous multiscale method. *Acta Numerica*, 21:1–87, 2012.

[2] S. Afkhami and M. Bussmann. Height functions for applying contact angles to 2d vof simulations. *International Journal for Numerical Methods in Fluids*, 57(4):453–472, 2008.

[3] S. Afkhami, S. Zaleski, and M. Bussmann. A mesh-dependent model for applying dynamic contact angles to vof simulations. *Journal of Computational Physics*, 228(15):5370 – 5389, 2009.

[4] W. Bangerth, R. Hartmann, and G. Kanschat. Deal.ii– a general-purpose object-oriented finite element library. *ACM Trans. Math. Softw.*, 33(4), Aug. 2007.

[5] W. Bangerth, T. Heister, L. Heltai, G. Kanschat, M. Kronbichler, M. Maier, B. Turcksin, and T. D. Young. The `deal.II` library, version 8.2. *Archive of Numerical Software*, 3, 2015.

[6] D. Bonn, J. Eggers, J. Indekeu, J. Meunier, and E. Rolley. Wetting and spreading. *Rev. Mod. Phys.*, 81:739–805, May 2009.

[7] H. Bruus. *Theoretical Microfluidics*. Oxford Master Series in Physics, 2007.

[8] J. W. Cahn and J. E. Hilliard. Free energy of a nonuniform system. i. interfacial free energy. *The Journal of Chemical Physics*, 28(2):258–267, 1958.

[9] R. G. Cox. The dynamics of the spreading of liquids on a solid surface. part 2. surfactants. *Journal of Fluid Mechanics*, 168:195–220, 7 1986.

[10] R. G. Cox. Inertial and viscous effects on dynamic contact angles. *Journal of Fluid Mechanics*, 357:249–278, 1998.

[11] P. G. de Gennes. Wetting: statics and dynamics. *Rev. Mod. Phys.*, 57:827–863, Jul 1985.

[12] M. Do-Quang, J. Shiomi, and G. Amberg. When and how surface structure determines the dynamics of partial wetting. *EPL (Europhysics Letters)*, 110(4):46002, 2015.

[13] J.-B. Dupont and D. Legendre. Numerical simulation of static and sliding drop with contact angle hysteresis. *Journal of Computational Physics*, 229(7):2453 – 2478, 2010.

[14] E. B. Dussan V. The moving contact line: the slip boundary condition. *Journal of Fluid Mechanics*, 77:665–684, 10 1976.

[15] E. B. Dussan V. and S. H. Davis. On the motion of a fluid-fluid interface along a solid surface. *Journal of Fluid Mechanics*, 65:71–95, 8 1974.

[16] W. E, B. Engquist, X. Li, W. Ren, and E. Vanden-Eijnden. Heterogeneous multiscale methods: A review. *Communications in Computational Physics*, 2(3):367–450, 2007.

[17] J. Eggers. Contact line motion for partially wetting fluids. *Physical Review E*, 72(6):061605, 2005.

[18] H. Elman, D. Silvester, and A. Wathen. *Finite Elements and Fast Iterative Solvers with Applications in Incompressible Fluid Dynamics*. Oxford Science Publications, Oxford, 2005.

[19] C. Galusinski and P. Vigneaux. On stability condition for bifluid flows with surface tension: Application to microfluidics. *Journal of Computational Physics*, 227(12):6140 – 6164, 2008.

[20] I. Ginzburg and G. Wittum. Two-phase flows on interface refined grids modeled with vof, staggered finite volumes, and spline interpolants. *Journal of Computational Physics*, 166(2):302 – 335, 2001.

[21] V. Girault and P.-A. Raviart. *Finite Element Methods for Navier-Stokes Equations. Theory and Algorithms.* Springer-Verlag, New York, 1986.

[22] J. Glimm, J. Grove, B. Lindquist, O. A. McBryan, and G. Tryggvason. The bifurcation of tracked scalar waves. *SIAM Journal on Scientific and Statistical Computing*, 9(1):61–79, 1988.

[23] P. M. Gresho and R. L. Sani. *Incompressible Flow and the Finite Element Method, volume two: Isothermal Laminar Flow*. John Wiley and Sons, 2000.

[24] J. Guermond, P. Minev, and J. Shen. An overview of projection methods for incompressible flows. *Computer Methods in Applied Mechanics and Engineering*, 195(44–47):6011 – 6045, 2006.

[25] C. Hirt and B. Nichols. Volume of fluid (vof) method for the dynamics of free boundaries. *Journal of Computational Physics*, 39(1):201 – 225, 1981.

[26] L. M. Hocking and A. D. Rivers. The spreading of a drop by capillary action. *Journal of Fluid Mechanics*, 121:425–442, 1982.

[27] C. Huh and L. Scriven. Hydrodynamic model of steady movement of a solid/ liquid/ fluid contact lin. *Journal of Colloid and Intarface Science*, 35(1), January 1971.

[28] D. Jacqmin. Calculation of two-phase navier–stokes flows using phase-field modeling. *Journal of Computational Physics*, 155(1):96 – 127, 1999.

[29] F. Y. Kafka and E. B. Dussan. On the interpretation of dynamic contact angles in capillaries. *Journal of Fluid Mechanics*, 95(3):539–565, 1979.

[30] M. Khenner. Computation of the material indicator function near the contact line (in tryggvason's method). *Journal of Computational Physics*, 200(1):1 – 7, 2004.

[31] J. Koplik, J. R. Banavar, and J. F. Willemsen. Molecular dynamics of fluid flow at solid surfaces. In M. Mareschal, editor, *Microscopic Simulations of Complex Flows*, volume 236 of *NATO ASI Series*, pages 99–128. Springer US, 1990.

[32] K. Kormann and M. Kronbichler. Parallel finite element operator application: Graph partitioning and coloring. In *Proc. 7th IEEE Int. Conf. eScience*, pages 332–339, 2011.

[33] M. Kronbichler. *Computational Techniques for Coupled Flow-Transport Problems*. PhD thesis, Uppsala University, Division of Scientific Computing, Numerical Analysis, 2011.

[34] M. Kronbichler and K. Kormann. A generic interface for parallel finite element operator application. *Comput. Fluids*, 63:135–147, 2012.

[35] M. Kronbichler and G. Kreiss. A phase-field microscale enhancement for macro models of capillary-driven contact point dynamics. *The Journal of Computational Multiphase Flows*, 0(0):1–13, 2017.

[36] D. Legendre and M. Maglio. Comparison between numerical models for the simulation of moving contact lines. *Computers & Fluids*, 113:2 – 13, 2015. Small scale simulation of multiphase flows.
[37] H. Liu, S. Krishnan, S. Marella, and H. Udaykumar. Sharp interface cartesian grid method ii: A technique for simulating droplet interactions with surfaces of arbitrary shape. *Journal of Computational Physics*, 210(1):32–54, 2005.
[38] K. Ljungkvist. *Finite Element Computations on Multicore and Graphics Processors*. PhD thesis, Uppsala University, Division of Scientific Computing, Numerical Analysis, 2017.
[39] G. Lu, X.-D. Wang, and Y.-Y. Duan. A critical review of dynamic wetting by complex fluids: From newtonian fluids to non-newtonian fluids and nanofluids. *Advances in Colloid and Interface Science*, 236:43 – 62, 2016.
[40] C. G. Ngan and E. B. D. V. On the dynamics of liquid spreading on solid surfaces. *Journal of Fluid Mechanics*, 209:191–226, 1989.
[41] E. Olsson and G. Kreiss. A conservative level set method for two phase flow. *Journal of Computational Physics*, 210(1):225 – 246, 2005.
[42] E. Olsson, G. Kreiss, and S. Zahedi. A conservative level set method for two phase flow ii. *J. Comput. Phys.*, 225(1):785–807, July 2007.
[43] S. Osher and J. A. Sethian. Fronts propagating with curvature-dependent speed: Algorithms based on hamilton-jacobi formulations. *Journal of Computational Physics*, 79(1):12 – 49, 1988.
[44] C. S. Peskin. Numerical analysis of blood flow in the heart. *Journal of Computational Physics*, 25(3):220 – 252, 1977.
[45] T. Qian, X.-P. Wang, and P. Sheng. Power-law slip profile of the moving contact line in two-phase immiscible flows. *Phys. Rev. Lett.*, 93:094501, Aug 2004.
[46] W. Ren and W. E. Heterogeneous multiscale method for the modeling of complex fluids and micro-fluidics. *Journal of Computational Physics*, 204(1):1 – 26, 2005.
[47] W. Ren and W. E. Boundary conditions for the moving contact line problem. *Physics of Fluids*, 19(2), 2007.
[48] M. Renardy, Y. Renardy, and J. Li. Numerical simulation of moving contact line problems using a volume-of-fluid method. *Journal of Computational Physics*, 171(1):243 – 263, 2001.
[49] W. J. Rider and D. B. Kothe. Reconstructing volume tracking. *Journal of Computational Physics*, 141(2):112 – 152, 1998.
[50] G. D. Rocca and G. Blanquart. Level set reinitialization at a contact line. *Journal of Computational Physics*, 265:34 – 49, 2014.
[51] Y. Saad. *Iterative Methods for Sparse Linear Systems*. SIAM, Philadelphia, second edition, 2003.
[52] J. A. Sethian. *Level set methods and fast marching methods*. Cambridge University Press, 1999.
[53] P. Sheng and M. Zhou. Immiscible-fluid displacement: Contact-line dynamics and the velocity-dependent capillary pressure. *Phys. Rev. A*, 45:5694–5708, Apr 1992.
[54] J. H. Snoeijer and B. Andreotti. Moving contact lines: Scales, regimes, and dynamical transitions. *Annual review of fluid mechanics*, 45:269 – 292, 2013.
[55] Z. Solomenko, P. D. Spelt, and P. Alix. A level-set method for large-scale

simulations of three-dimensional flows with moving contact lines. *Journal of Computational Physics*, 348:151 – 170, 2017.

[56] P. D. Spelt. A level-set approach for simulations of flows with multiple moving contact lines with hysteresis. *Journal of Computational Physics*, 207(2):389 – 404, 2005.

[57] Y. Sui, H. Ding, and P. D. Spelt. Numerical simulations of flows with moving contact lines. *Annual Review of Fluid Mechanics*, 46(1):97–119, 2014.

[58] Y. Sui and P. D. Spelt. An efficient computational model for macroscale simulations of moving contact lines. *Journal of Computational Physics*, 242:37 – 52, 2013.

[59] M. Sussman and E. G. Puckett. A coupled level set and volume-of-fluid method for computing 3d and axisymmetric incompressible two-phase flows. *Journal of Computational Physics*, 162(2):301 – 337, 2000.

[60] M. Sussman, P. Smereka, and S. Osher. A level set approach for computing solutions to incompressible two-phase flow. *Journal of Computational Physics*, 114(1):146 – 159, 1994.

[61] X.-P. W. Tiezheng Qian and P. Sheng. Molecular hydrodynamics of the moving contact line in two-phase immiscible flows. *Communications in Computational Physics*, 1(1), February 2006.

[62] G. Tryggvason, R. Scardovelli, and S. Zaleski. *Direct numerical simulations of gas-liquid multiphase flows.* Cambridge University Press., Cambridge, 2011.

[63] S. O. Unverdi and G. Tryggvason. A front-tracking method for viscous, incompressible, multi-fluid flows. *Journal of Computational Physics*, 100(1):25 – 37, 1992.

[64] L. R. Volpatti and A. K. Yetisen. Commercialization of microfluidic devices. *Trends in Biotechnology*, 32(7):347 – 350, 2014.

[65] J.-J. Xu and W. Ren. A level-set method for two-phase flows with moving contact line and insoluble surfactant. *Journal of Computational Physics*, 263:71 – 90, 2014.

[66] K. Yokoi, D. Vadillo, J. Hinch, and I. Hutchings. Numerical studies of the influence of the dynamic contact angle on a droplet impacting on a dry surface. *Physics of Fluids*, 21(7), 2009.

[67] P. Yue, C. Zhou, and J. J. Feng. Sharp-interface limit of the cahn–hilliard model for moving contact lines. *Journal of Fluid Mechanics*, 645:279–294, 2 2010.

[68] S. Zahedi. *Numerical Methods for Fluid Interface Problems*. PhD thesis, KTH, Numerical Analysis, NA, 2011. QC 20110503.

Acta Universitatis Upsaliensis

Digital Comprehensive Summaries of Uppsala Dissertations from the Faculty of Science and Technology 1559

Editor: The Dean of the Faculty of Science and Technology

A doctoral dissertation from the Faculty of Science and Technology, Uppsala University, is usually a summary of a number of papers. A few copies of the complete dissertation are kept at major Swedish research libraries, while the summary alone is distributed internationally through the series Digital Comprehensive Summaries of Uppsala Dissertations from the Faculty of Science and Technology. (Prior to January, 2005, the series was published under the title "Comprehensive Summaries of Uppsala Dissertations from the Faculty of Science and Technology".)

Distribution: publications.uu.se
urn:nbn:se:uu:diva-329059

ACTA
UNIVERSITATIS
UPSALIENSIS
UPPSALA
2017